nature medicine

Rationale for co-targeting IGF-1R and ALK in *ALK* fusion–positive lung cancer

Christine M Lovly[1], Nerina T McDonald[1], Heidi Chen[2], Sandra Ortiz-Cuaran[3], Lukas C Heukamp[4,5], Yingjun Yan[1], Alexandra Florin[4], Luka Ozretić[4], Diana Lim[6], Lu Wang[6], Zhao Chen[7], Xi Chen[2], Pengcheng Lu[2], Paul K Paik[8], Ronglai Shen[9], Hailing Jin[1], Reinhard Buettner[4], Sascha Ansén[10], Sven Perner[11], Michael Brockmann[12], Marc Bos[3,10], Jürgen Wolf[10], Masyar Gardizi[10], Gavin M Wright[13], Benjamin Solomon[14], Prudence A Russell[15], Toni-Maree Rogers[16], Yoshiyuki Suehara[6], Monica Red-Brewer[1], Rudy Tieu[17], Elisa de Stanchina[17], Qingguo Wang[18], Zhongming Zhao[18], David H Johnson[19], Leora Horn[1], Kwok-Kin Wong[7], Roman K Thomas[3,4], Marc Ladanyi[6] & William Pao[1]

Crizotinib, a selective tyrosine kinase inhibitor (TKI), shows marked activity in patients whose lung cancers harbor fusions in the gene encoding anaplastic lymphoma receptor tyrosine kinase (ALK), but its efficacy is limited by variable primary responses and acquired resistance. In work arising from the clinical observation of a patient with *ALK* fusion–positive lung cancer who had an exceptional response to an insulin-like growth factor 1 receptor (IGF-1R)-specific antibody, we define a therapeutic synergism between ALK and IGF-1R inhibitors. Similar to IGF-1R, ALK fusion proteins bind to the adaptor insulin receptor substrate 1 (IRS-1), and IRS-1 knockdown enhances the antitumor effects of ALK inhibitors. In models of ALK TKI resistance, the IGF-1R pathway is activated, and combined ALK and IGF-1R inhibition improves therapeutic efficacy. Consistent with this finding, the levels of IGF-1R and IRS-1 are increased in biopsy samples from patients progressing on crizotinib monotherapy. Collectively these data support a role for the IGF-1R–IRS-1 pathway in both ALK TKI–sensitive and ALK TKI–resistant states and provide a biological rationale for further clinical development of dual ALK and IGF-1R inhibitors.

Genomic alterations in *ALK* are found in numerous malignancies[1]. In a phase 1 trial, the ALK TKI crizotinib induced an objective radiographic response (ORR) of 60.8% and a median progression-free survival of 9.7 months in patients with *ALK* fusion–positive (ALK$^+$) lung cancer[2]. Unfortunately, patients invariably developed therapeutic resistance. The mechanisms of resistance to ALK blockade are only beginning to be elucidated[3–6].

Analysis of 'exceptional responders' has revealed important insights into drug sensitivity[7]. We describe a patient with ALK$^+$ lung cancer who had an exceptional response to an IGF-1R inhibitor before ALK TKI therapy. Using this patient as a paradigm of an exceptional responder, we uncovered an association between IGF-1R and IRS-1 and ALK signaling. Collectively our studies suggest that this rationally selected combination of inhibitors may be an effective strategy to delay or overcome resistance to therapeutic ALK inhibition.

RESULTS

Exceptional response to an IGF-1R inhibitor

A 50-year-old female with stage 4 lung adenocarcinoma received standard first-line platinum-based chemotherapy. She then enrolled in a clinical trial of erlotinib followed at progression by erlotinib plus an IGF-1R–specific monoclonal antibody (mAb). At the time of enrollment, her tumor mutation status was unknown. She developed progressive disease after 1 month of erlotinib treatment (**Fig. 1a**,**b**). Per the trial protocol, the IGF-1R mAb was added to her treatment, and she then experienced a partial response lasting 17 months (**Fig. 1c**).

[1]Department of Medicine, Vanderbilt University, Nashville, Tennessee, USA. [2]Department of Biostatistics, Vanderbilt University, Nashville, Tennessee, USA. [3]Department of Translational Genomics, Center of Integrated Oncology Köln-Bonn, University Hospital Cologne, Cologne, Germany. [4]Department of Pathology, Center for Integrated Oncology Köln-Bonn, University Hospital Cologne, Cologne, Germany. [5]New Oncology, Cologne, Germany. [6]Department of Pathology, Memorial Sloan Kettering Cancer Center, New York, New York, USA. [7]Department of Medical Oncology, Dana-Farber Cancer Institute, Boston, Massachusetts, USA. [8]Department of Medicine, Memorial Sloan Kettering Cancer Center, New York, New York, USA. [9]Department of Epidemiology and Biostatistics, Memorial Sloan Kettering Cancer Center, New York, New York, USA. [10]Department of Internal Medicine (Department I), Center for Integrated Oncology Köln-Bonn, University Hospital Cologne, Cologne, Germany. [11]Department of Prostate Cancer Research, Institute of Pathology, Center of Integrated Oncology Köln-Bonn, University Hospital of Bonn, Bonn, Germany. [12]Department of Pathology, Hospital Merheim, Cologne, Germany. [13]Department of Surgery, University of Melbourne, St. Vincent's Hospital, Melbourne, Victoria, Australia. [14]Division of Hematology and Medical Oncology, Peter MacCallum Cancer Center, Melbourne, Australia. [15]Department of Anatomical Pathology, St. Vincent's Hospital, Melbourne, Victoria, Australia. [16]Department of Pathology, Peter MacCallum Cancer Center, Melbourne, Victoria, Australia. [17]Anti-tumor Assessment Core Facility, Memorial Sloan Kettering Cancer Center, New York, New York, USA. [18]Department of Biomedical Informatics, Vanderbilt University, Nashville, Tennessee, USA. [19]Department of Medicine, UT Southwestern School of Medicine, Dallas, Texas, USA. Correspondence should be addressed to C.M.L. (christine.lovly@vanderbilt.edu).

Received 27 January; accepted 23 July; published online 31 August 2014; doi:10.1038/nm.3667

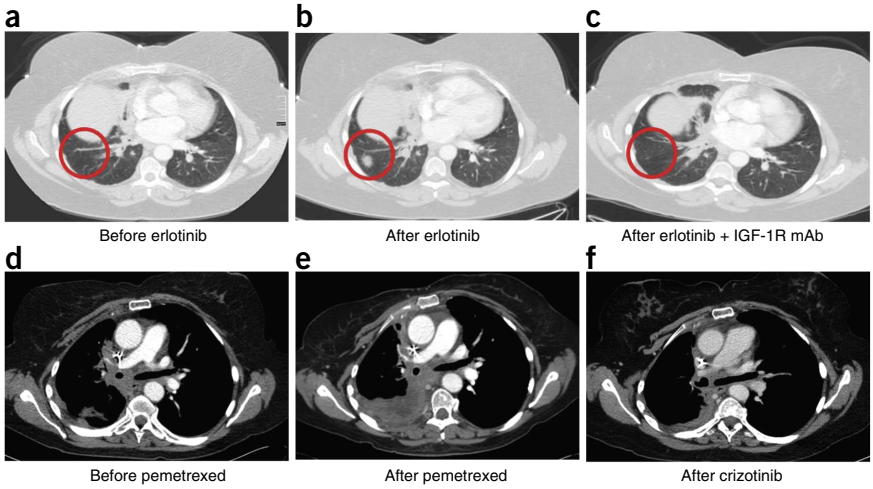

Figure 1 Exceptional response to an IGF-1R inhibitor before ALK TKI therapy in a patient with ALK+ lung cancer. Representative images from serial computed tomography scans of the chest of a 50-year-old female with ALK+ lung cancer documenting responses to the therapies indicated. Images are labeled **a**–**f** in temporal sequence. The red circles in **a**–**c** represent a new lesion in the right lung that developed after 1 month of erlotinib and then responded to erlotinib plus an IGF-1R–specific antibody. The scale bar in **Figure 1a** indicates 4 cm and is representative for all images.

She remained on this treatment longer than any other patient enrolled in the trial.

At the time of progression on erlotinib plus the IGF-1R mAb, the patient's tumor was sent for molecular profiling. As expected based on the lack of response to erlotinib, the tumor did not contain an *EGFR* mutation (**Supplementary Table 1**); surprisingly, however, it did harbor an *ALK* rearrangement. Subsequently, this patient enrolled in the phase 3 trial of crizotinib compared to chemotherapy (profile 1007, NCT00932893) and was randomized to pemetrexed, a folate antimetabolite. After four cycles, she had disease progression (**Fig. 1d**,**e**), started on crizotinib per the trial protocol and had a partial response (**Fig. 1f**).

Previous studies have reported a 0% response rate for patients with ALK+ lung cancer treated with erlotinib alone[8]. Thus, we hypothesized that in this patient, either the combination of erlotinib plus the IGF-1R inhibitor was synergistic against ALK+ lung cancer or the IGF-1R inhibitor alone was somehow responsible for the tumor response. To address this hypothesis, we treated H3122 cells, which harbor an *EML4-ALK* E13;A20 fusion (where E13;A20 refers to the exons in *EML4* (E) that are fused to *ALK* (A)), with erlotinib, an IGF-1R TKI or MAb alone

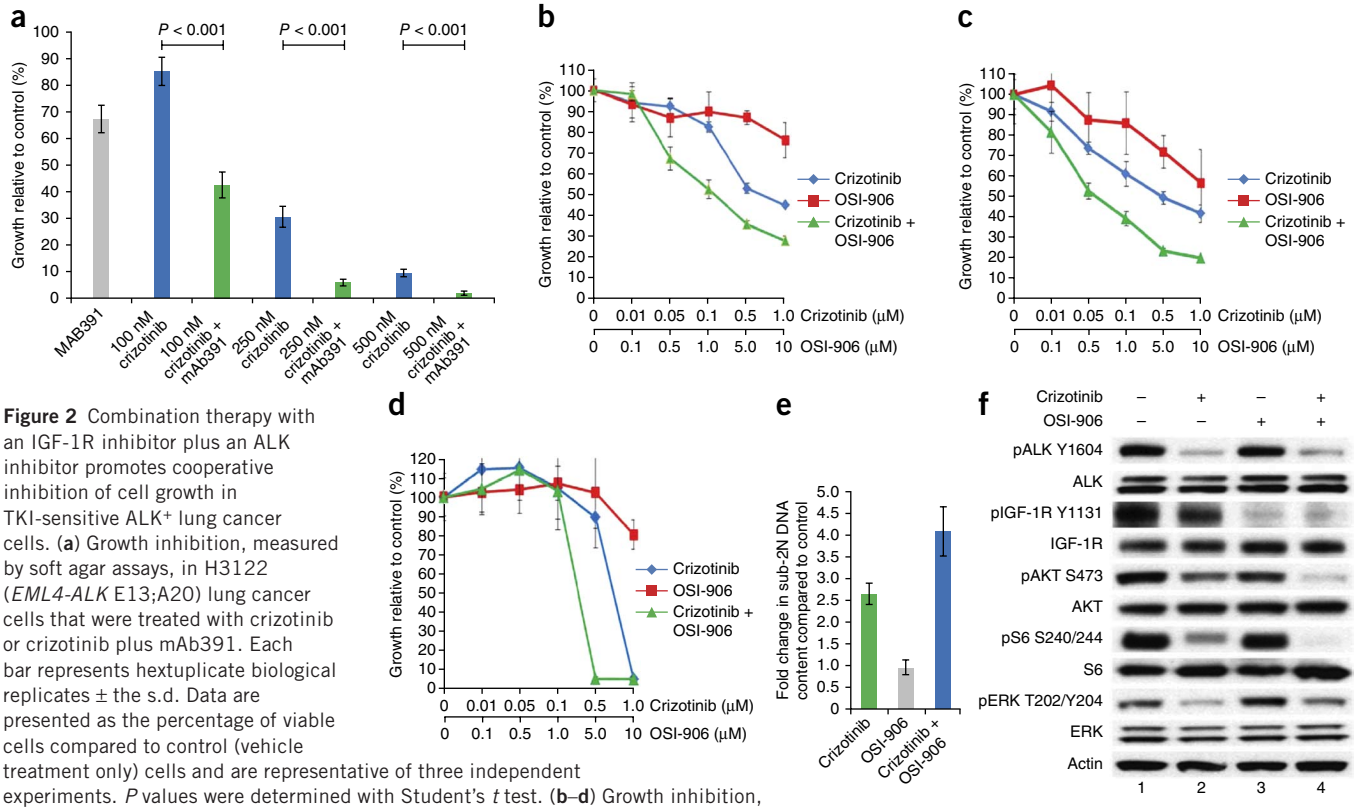

Figure 2 Combination therapy with an IGF-1R inhibitor plus an ALK inhibitor promotes cooperative inhibition of cell growth in TKI-sensitive ALK+ lung cancer cells. (**a**) Growth inhibition, measured by soft agar assays, in H3122 (*EML4-ALK* E13;A20) lung cancer cells that were treated with crizotinib or crizotinib plus mAb391. Each bar represents hextuplicate biological replicates ± the s.d. Data are presented as the percentage of viable cells compared to control (vehicle treatment only) cells and are representative of three independent experiments. *P* values were determined with Student's *t* test. (**b**–**d**) Growth inhibition, assessed by cell titer blue assays, of H3122 (*EML4-ALK* E13;A20) (**b**), H2228 (*EML4-ALK* 6a/b;A20) (**c**) and STE-1 (*EML4-ALK* E13;A20) (**d**) lung cancer cells that were treated with increasing amounts of crizotinib, OSI-906 or the combination for 72 h. Each point represents hextuplicate biological replicates ± s.d. Data are presented as the percentage of viable cells compared to control (vehicle treatment only) cells and are representative of three or more independent experiments. (**e**) Cell numbers, determined by staining with propidium iodide (PI) and counting on a FACSCalibur machine, of STE-1 cells that were treated with one dose of 1 μM crizotinib, 2 μM OSI-906 or the combination for a total of 72 h before harvest. Each point represents triplicate biological replicates ± s.d. (**f**) Immunoblot analysis using antibodies specific to the proteins indicated of lysates of H3122 cells that were treated with crizotinib, OSI-906 or the combination for 2 h before harvest. Select images were quantified using a Bio-Rad Gel Doc XR and Image Lab software (**Supplementary Figs. 1i** and **2b**). This experiment was repeated three independent times.

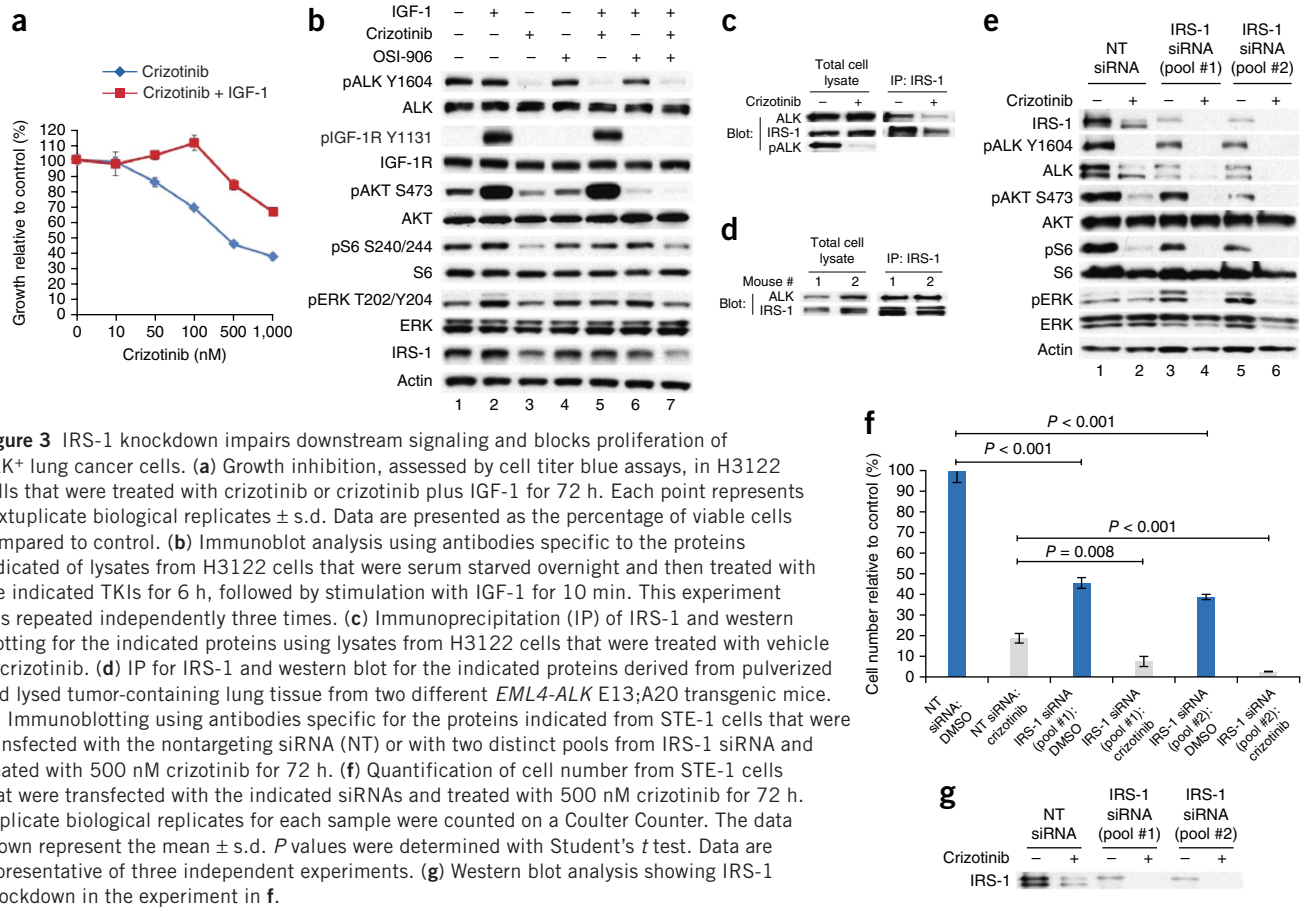

Figure 3 IRS-1 knockdown impairs downstream signaling and blocks proliferation of ALK+ lung cancer cells. (**a**) Growth inhibition, assessed by cell titer blue assays, in H3122 cells that were treated with crizotinib or crizotinib plus IGF-1 for 72 h. Each point represents hextuplicate biological replicates ± s.d. Data are presented as the percentage of viable cells compared to control. (**b**) Immunoblot analysis using antibodies specific to the proteins indicated of lysates from H3122 cells that were serum starved overnight and then treated with the indicated TKIs for 6 h, followed by stimulation with IGF-1 for 10 min. This experiment was repeated independently three times. (**c**) Immunoprecipitation (IP) of IRS-1 and western blotting for the indicated proteins using lysates from H3122 cells that were treated with vehicle or crizotinib. (**d**) IP for IRS-1 and western blot for the indicated proteins derived from pulverized and lysed tumor-containing lung tissue from two different *EML4-ALK* E13;A20 transgenic mice. (**e**) Immunoblotting using antibodies specific for the proteins indicated from STE-1 cells that were transfected with the nontargeting siRNA (NT) or with two distinct pools from IRS-1 siRNA and treated with 500 nM crizotinib for 72 h. (**f**) Quantification of cell number from STE-1 cells that were transfected with the indicated siRNAs and treated with 500 nM crizotinib for 72 h. Triplicate biological replicates for each sample were counted on a Coulter Counter. The data shown represent the mean ± s.d. *P* values were determined with Student's *t* test. Data are representative of three independent experiments. (**g**) Western blot analysis showing IRS-1 knockdown in the experiment in **f**.

or the combination. We observed no therapeutic synergism between erlotinib and the IGF-1R inhibitors (**Supplementary Fig. 1a**,**b**), suggesting that this patient's tumor response was more likely due to the IGF-1R–specific antibody. On the basis of this clinical observation, we hypothesized that there is crosstalk between IGF-1R and ALK that may be exploited therapeutically to improve antitumor responses.

Therapeutic synergism between ALK and IGF-1R inhibitors

We tested the ability of IGF-1R inhibitors alone or in combination with ALK inhibitors to impede the growth of ALK+ lung cancer cell lines. The IGF-1R–specific mAb, mAb391, had modest but reproducible single-agent activity in H3122 cells. However, mAb391 sensitized H3122 cells to the antiproliferative effects of crizotinib (**Fig. 2a**). When we inhibited IGF-1R with mAb391, sensitivity to crizotinib was also enhanced in STE-1 (*EML4-ALK* E13;A20) cells, a new lung adenocarcinoma cell line that we developed from a patient with ALK+ lung cancer (**Supplementary Fig. 1c**). We observed similar results when we treated H3122 cells with the dual IGF-1R and insulin receptor TKI OSI-906 plus crizotinib (**Fig. 2b**). We extended this finding to other ALK+ lung cancer cell lines, including H2228 (*EML4-ALK* E6a/b;A20) (**Fig. 2c**) and STE-1 (**Fig. 2d**). Co-treatment with an ALK TKI plus an IGF-1R TKI also induced better antitumor responses in SUDHL-1 lymphoma cells, which harbor an *NPM-ALK* fusion, suggesting that this effect is not specific to ALK-mutant lung cancer cells (**Supplementary Fig. 1e**). We confirmed the combination of crizotinib plus OSI-906 to be synergistic using the Mix-Low method[9], which is a standard mathematical model to assess drug-drug interactions (**Supplementary Fig. 1d**). OSI-906 has no off-target activity against ALK at the doses used in these experiments[10].

Compared to crizotinib alone, the combination of crizotinib plus OSI-906 resulted in increased levels of apoptosis (**Fig. 2e**) and decreased phosphorylation of downstream targets (**Fig. 2f**). Furthermore, the combination of crizotinib plus mAb391 was more effective at delaying the growth of ALK+ xenografts in nude (*nu/nu*) mice (**Supplementary Fig. 1f**). Collectively these data show that the combination of ALK plus IGF-1R inhibitors results in an enhanced antiproliferative response in ALK+ lung cancer cells.

To ascertain the specificity of this effect, we examined whether inhibitors of other tyrosine kinases could produce analogous results. Neither the epidermal growth factor receptor (EGFR) inhibitor erlotinib (**Supplementary Fig. 1g**) nor the dual HER2 (also called ERBB2) and EGFR inhibitor lapatinib (**Supplementary Fig. 1h**) was able to sensitize H3122 cells to the effects of crizotinib. These data suggest that the synergistic antiproliferative effect described above is specific to IGF-1R blockade.

To assess whether ligand-induced activation of IGF-1R could influence the antiproliferative effects of ALK blockade, we treated H3122 cells with crizotinib alone or in combination with IGF-1. The addition of IGF-1 induced resistance to the growth-inhibitory effects of crizotinib (**Fig. 3a**). IGF-1 ligand stimulated phosphorylation of IGF-1R but not ALK (**Fig. 3b** and **Supplementary Fig. 2a**), suggesting no direct crosstalk between the two kinases. When we stimulated cells pretreated with crizotinib with IGF-1, ALK phosphorylation was inhibited; however, downstream signaling was sustained, as evidenced by continued phosphorylation of AKT (**Fig. 3b**). OSI-906 was able to inhibit this response. Taken together, these data suggest that signaling through IGF-1R may be a compensatory mechanism for the growth-inhibitory effects of ALK inhibitor therapy.

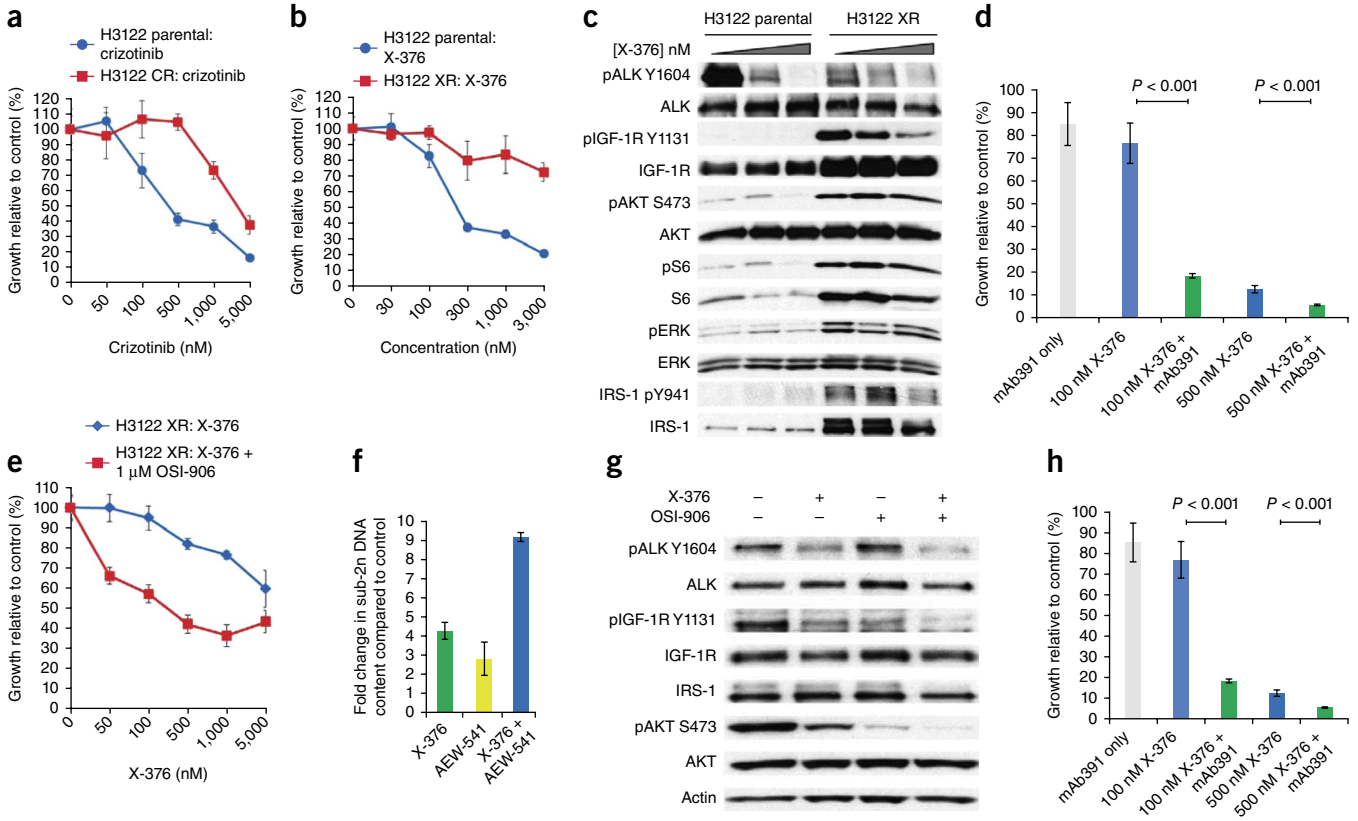

Figure 4 The IGF-1R pathway is activated in models of ALK TKI resistance. (**a**,**b**) Cell titer blue assays of isogenic pairs of H3122 parental (i.e., TKI sensitive), CR, or XR cells that were treated with crizotinib (**a**) or X-376 (**b**). Data represent hextuplicate biological replicates ± s.d. The data shown are representative of 3 independent experiments. (**c**) Immunoblotting using antibodies specific for the proteins indicated of lysates from H3122 XR cells that were treated with X-376 for 4 h. This experiment was repeated two independent times. (**d**) Soft agar assays of H3122 XR cells that were treated with X-376 or X-376 plus mAb391. Data represent hextuplicate biological replicates ± s.d. and are representative of two independent experiments. (**e**) Cell titer blue assays of H3122 XR cells that were treated with X-376 or X-376 plus OSI-906 for 72 h. Data represent hextuplicate biological replicates ± s.d. and are representative of three independent experiments. (**f**) Numbers of H3122 XR cells, determined by staining with PI and counting on a FACSCanto II machine, that were treated with X-376, AEW-541 or the combination daily for 72 h. Each point represents triplicate biological replicates ± s.d. (**g**) Immunoblotting using antibodies specific for the proteins indicated of lysates of H3122 XR cells that were treated with the indicated inhibitors for 4 h. (**h**) Quantification of cell number from H3122 XR cells that were transfected with the indicated siRNAs and treated with 500 nM X-376 for 72 h. Quadruplicate biological replicates for each sample were counted on a Coulter Counter. Data are representative of three independent experiments. (**i**) Western blot analysis confirming IRS-1 knockdown in the experiment in **h**. All *P* values shown were determined with Student's *t* test.

IRS-1 knockdown impedes growth of ALK+ lung cancer cells

We investigated the molecular mechanisms underlying the cooperative antitumor response between ALK and IGF-1R inhibitors. IRS-1 is a well-known substrate and adaptor protein for IGF-1R[11], and IRS-1 has been demonstrated to be a primary adaptor for phosphatidylinositol-4,5-bisphosphate 3-kinase (PI3K) activation in H3122 cells[12]. However, the precise mechanism by which ALK fusion proteins link to effector pathways remains undefined. We observed that IRS-1 levels decreased with crizotinib treatment (**Fig. 3b**). Using lysates from H3122 cells, we found that ALK and IRS-1 coimmunoprecipitated and that the interaction decreased after the addition of crizotinib (**Fig. 3c**). We also validated that this interaction occurs *in vivo* using lung tumor tissue from two different *EML4-ALK* E13;A20 transgenic mice[13] (**Fig. 3d**).

Next we hypothesized that if IRS-1 is an adaptor protein for ALK, then knockdown of IRS-1 would sensitize cells to the effects of ALK inhibition. Consistent with our hypothesis, IRS-1 knockdown sensitized STE-1 cells to the effects of crizotinib (**Fig. 3e**). The levels of phosphorylated AKT, S6 and ERK were lower in IRS-1 siRNA–transfected, crizotinib-treated cells compared to crizotinib-treated controls. IRS-1 knockdown impaired the proliferation of STE-1 cells in the absence of crizotinib and also sensitized these cells to the antiproliferative effects of ALK inhibition (**Fig. 3f**,**g**). We observed analogous results in H2228 cells (**Supplementary Fig. 3a**,**b**). Taken together, these data suggest that IRS-1 is an adaptor protein that links both IGF-1R and ALK to downstream signaling pathways.

IGF-1R pathway upregulation in ALK TKI–resistant cells

Our data suggest that increased signaling through IGF-1R, after stimulation with exogenous IGF-1 ligand, decreases cellular dependence on ALK, as indicated by diminished sensitivity to ALK TKIs (**Fig. 3a**,**b**). Understanding the signaling of an oncogene can also help provide an

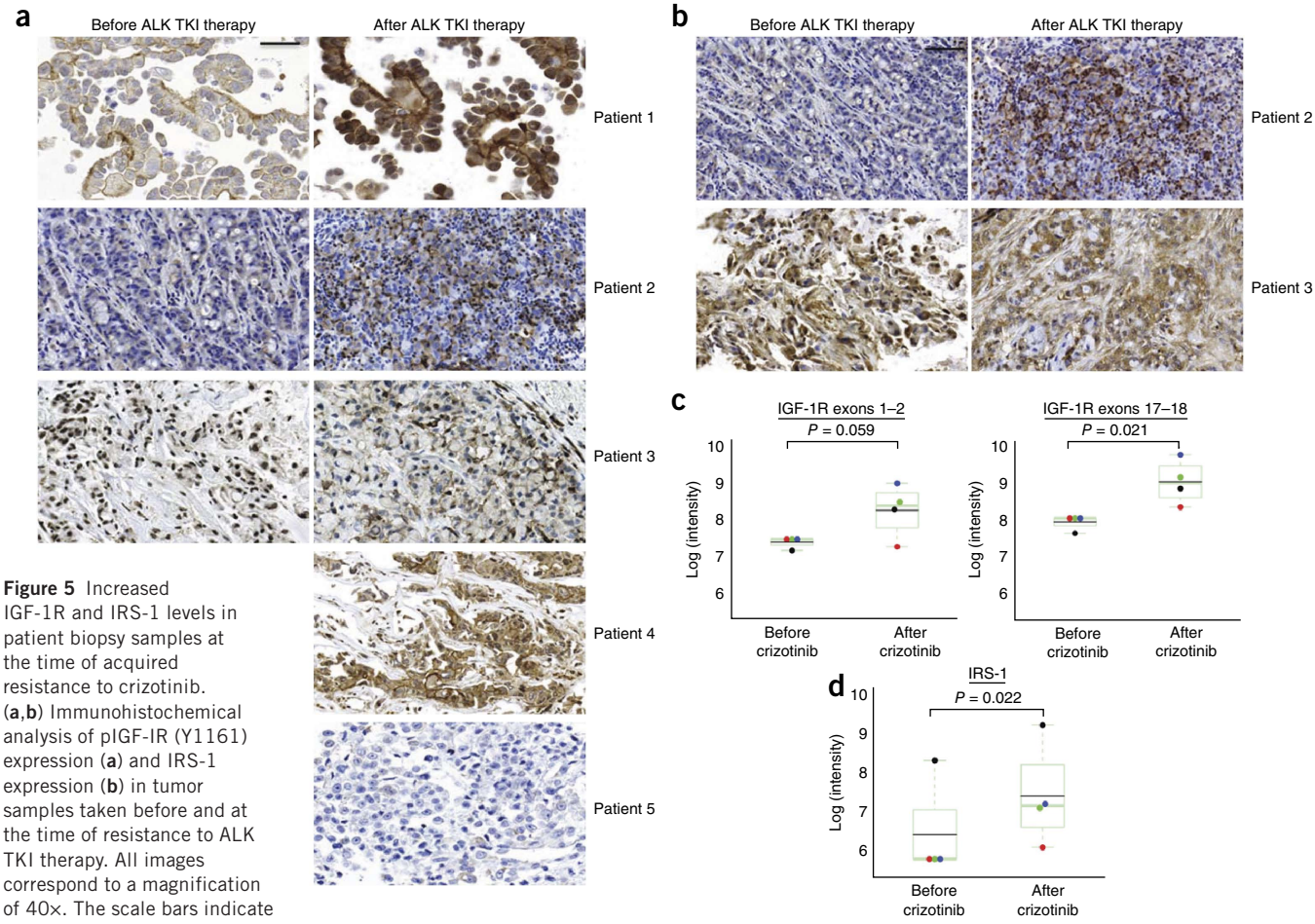

Figure 5 Increased IGF-1R and IRS-1 levels in patient biopsy samples at the time of acquired resistance to crizotinib. (**a**,**b**) Immunohistochemical analysis of pIGF-IR (Y1161) expression (**a**) and IRS-1 expression (**b**) in tumor samples taken before and at the time of resistance to ALK TKI therapy. All images correspond to a magnification of 40×. The scale bars indicate 200 μm. (**c**,**d**) Expression levels of IGF-1R (**c**) and IRS-1 (**d**) before and after crizotinib treatment in RNA that was extracted from formalin-fixed, paraffin-embedded tumor biopsy samples before and at the time of progressive disease on crizotinib and run on the NanoString assay. NanoString target sequences for IGF-1R have been previously reported[23]. The colored dots within each box plot represent distinct pairs of matched before- and after-crizotinib samples. The black dots indicate the patient sample. The red dots and the green dots represent H3122 parental (TKI-sensitive) cells compared with H3122 CR cells at 1× crizotinib resistance (1 μM final concentration of crizotinib, red dot) or H3122 CR cells at 2× crizotinib resistance (2 μM final concentration of crizotinib, green dot). The blue dots represent H3122 parental compared with H3122 XR cells. The green horizontal line represents the median, and the black horizontal line represents the mean. *P* values were determined with a modified paired *t* test using the limma package.

understanding of how therapeutic resistance develops. We therefore modeled ALK TKI resistance *in vitro*. Starting with drug-sensitive (parental) cells, we derived H3122 cells that were resistant to crizotinib (**Fig. 4a**) or to X-376 (**Fig. 4b**), which is a more potent and more specific ALK inhibitor[14]. Notably, a derivative of X-376 (X-396) is currently in phase 1 clinical trials in patients with advanced solid tumors (NCT01625234). We analyzed these resistant cell lines using a variety of methods. H3122 crizotinib-resistant (H3122 CR) cells displayed amplification of the *EML4-ALK* E13;A20 fusion by *ALK* fluorescence *in situ* hybridization (FISH) (**Supplementary Fig. 4a**,**b**), as described previously[15]. These cells did not have any second-site ALK kinase domain mutations (data not shown).

H3122 X376-resistant (H3122 XR) cells harbored neither *ALK* amplification (**Supplementary Fig. 4c**) nor second-site mutations. However, H3122 XR cells maintained phosphorylation of AKT, S6 and ERK even in the continued presence of X-376 (**Fig. 4c**). We hypothesized that an alternative upstream kinase(s) must be activated in these cells to maintain signaling. Phospho–receptor tyrosine kinase (RTK) arrays revealed an increase in IGF-1R phosphorylation (**Supplementary Fig. 4d**). Indeed, IGF-1R phosphorylation and total protein levels were elevated in the ALK TKI–resistant compared to the ALK TKI–sensitive (i.e., parental) cells (**Fig. 4c**). H3122 XR cells also exhibited increased phosphorylation and total protein levels of IRS-1. Overall these results suggest that the IGF-1R–IRS-1 pathway has a role in maintaining downstream signaling in the presence of continuous ALK inhibition and may therefore be a mechanism by which cells evade ALK blockade.

We next sought to determine how IGF-1 signaling is upregulated in ALK TKI–resistant cells. IGF-1 ligand levels were increased in the conditioned medium from H3122 XR cells (**Supplementary Fig. 4d**). Gene expression profiling revealed that IGF binding protein 3 (IGFBP3) was downregulated in resistant compared to parental cells (**Supplementary Tables 2** and **3**). IGFBP3 is known to block IGF-1–induced activation of IGF-1R[16,17]. Overall these studies show that the IGF-1R signaling pathway is activated by multiple mechanisms in H3122 XR cells.

We evaluated the effects of IGF-1R inhibition in ALK TKI–resistant cells. The combination of X-376 with either mAb391 or OSI-906 (**Fig. 4d**,**e**) partially restored X-376 sensitivity in H3122 XR cells. Apoptosis was also enhanced in H3122 XR cells treated with X-376

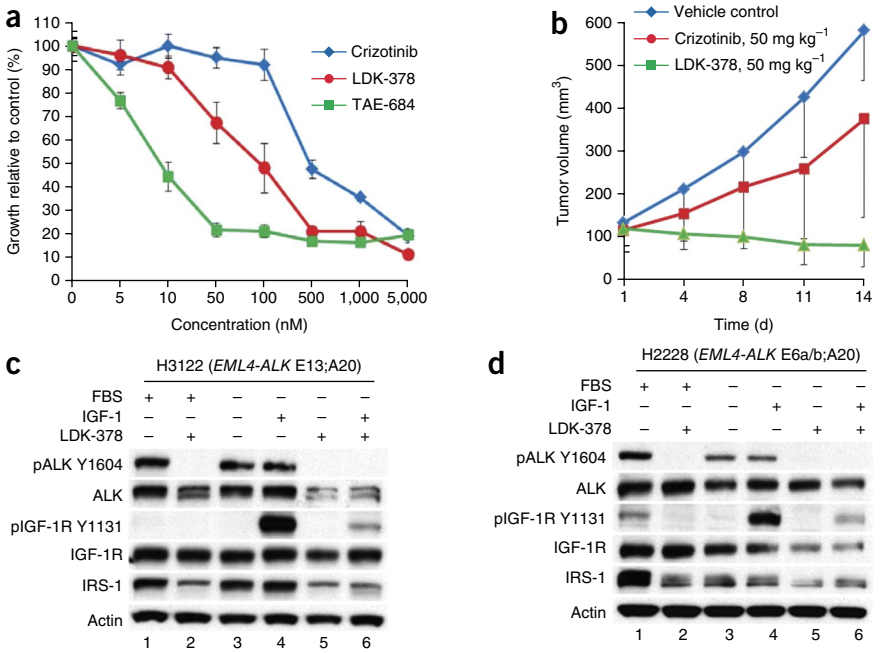

Figure 6 The second-generation ALK inhibitor LDK-378 blocks the phosphorylation of both ALK and IGF-1R. (**a**) Cell growth inhibition, assessed by cell titer blue assays, of H3122 lung cancer cells containing the *EML4-ALK* E13;A20 fusion that were treated with increasing amounts of crizotinib, LDK-378 or TAE-684 for 72 h. Each point represents hextuplicate biological replicates ± s.d. Data are presented as the percentage of viable cells compared to control (vehicle treatment only) cells and are representative of three or more independent experiments. (**b**) Tumor volumes, assessed every 3–4 days, in athymic *nu/nu* female mice that were injected subcutaneously with H3122 lung cancer cells harboring the *EML4-ALK* E13;A20 fusion. When tumors reached an average volume of 100 mm^3, mice were randomized to receive crizotinib alone (50 mg per kg body weight by mouth (p.o.) daily for 5 d), LDK-378 alone (50 mg per kg body weight p.o. daily for 5 d) or vehicle control ($n = 5$ for crizotinib, and LDK-378, $n = 4$ for vehicle control). Data represent the mean tumor volume ± s.d. $P = 0.0159$ based on the Wilcoxon rank-sum test for the comparison between crizotinib and LDK-378. (**c**,**d**) Immunoblotting using antibodies specific for the proteins indicated of lysates from H3122 (**c**) and H2228 cells (**d**) that were grown overnight in the presence or absence of serum and then treated with LDK-378 for 1 h, followed by stimulation with IGF-1 for 10 min and harvesting. This experiment was repeated three independent times.

and the IGF-1R TKI AEW-541 (ref. 18) (**Fig. 4f**). In accord with these data, combination treatment with ALK and IGF-1R inhibitors in H3122 XR cells inhibited AKT phosphorylation to a greater extent than treatment with either inhibitor alone (**Fig. 4g**). The addition of OSI-906 also partially restored the sensitivity of H3122 CR cells to the growth-inhibitory effects of crizotinib (**Supplementary Fig. 4c**).

Because IRS-1 levels were increased in H3122 XR cells (**Fig. 4c**), we examined whether IRS-1 knockdown would also affect signaling and proliferation in the resistant cells (**Fig. 4h**,**i**). We transfected H3122 XR cells with IRS-1 or control siRNAs and then treated them with X-376. IRS-1 knockdown sensitized these cells to the antiproliferative effects of ALK inhibition (**Fig. 4h**) and resulted in a further decline in the phosphorylation of downstream targets compared to X-376 treatment alone or IRS-1 knockdown alone (**Fig. 4i**).

Previous studies have suggested that the IGF-1R pathway can drive EGFR inhibitor resistance[19,20]. We tested the efficacy of combined EGFR and IGF-1R inhibition in four different isogenic pairs of EGFR TKI–sensitive and EGFR TKI–resistant cell lines[21,22] (**Supplementary Table 4**). The addition of the IGF-1R TKI OSI-906 was not synergistic with the EGFR TKI erlotinib in any of these cells (**Supplementary Fig. 5a–d**). Furthermore, in contrast to the ALK TKI–resistant cells, there was no increase in IGF-1R or IRS-1 levels in the EGFR TKI–resistant cell lines (**Supplementary Fig. 5e**). Therefore, because there was no therapeutic synergism between EGFR and IGF-1R inhibitors in EGFR-mutant lung cancer cell lines, these data suggest that the synergistic effects seen with the ALK and IGF-1R inhibitor combinations in the ALK cell lines are true differences.

Increased IGF-1R in tumor samples at the time of resistance

To validate the clinical implications of our *in vitro* findings, we evaluated the levels of phosphorylated IGF-1R (pIGF-1R) and IRS-1 in patient lung cancer biopsy samples. We examined three sets of paired tumor samples before and after crizotinib treatment, as well as two tumor samples after crizotinib treatment from five different patients, by immunohistochemistry (IHC) for pIGF-1R. These samples were then blindly evaluated by pathologists. As a control, we also performed pIGF-1R IHC on lung cancer tissue microarrays (representative examples are shown in **Supplementary Fig. 6a–c**). Four of five tumor biopsies taken at the time of acquired resistance displayed increased levels of pIGF-1R (**Fig. 5a**). For two of the paired tumor samples, we had sufficient tissue to examine IRS-1 levels by IHC (**Fig. 5b**); one sample after treatment (patient 2) had increased IRS-1 expression. We also assessed these five samples for ALK kinase domain mutations that are associated with crizotinib resistance (**Supplementary Table 5**). Patient 4's tumor after crizotinib treatment harbored an ALK G1202R mutation in the kinase domain.

As an orthogonal approach, we performed mRNA expression analysis for *IGF1R* and *IRS1* using NanoString[23] on matched patient samples and on isogenic pairs of ALK TKI–sensitive and ALK TKI–resistant cell lines. In the one case with enough tissue available for analysis before and after treatment, *IGF1R* and *IRS1* (**Fig. 5c,d**) mRNA levels were increased in the tumor sample after crizotinib treatment relative to the sample before treatment. We obtained similar results with the cell lines. In contrast, NanoString analysis of 11 matched pairs of EGFR-mutant lung tumor biopsies revealed no significant change in IRS-1 levels after EGFR TKI therapy (**Supplementary Fig. 6d–f**), suggesting that the changes observed in IRS-1 were specific to ALK^+ lung cancer. Overall these data validate our preclinical findings, showing that levels of IGF-1R and IRS-1 can be increased after ALK TKI therapy in patient-derived samples.

LDK-378 inhibits phosphorylation of ALK and IGF-1R *in vitro*

The second-generation ALK TKI LDK-378 (ceritinib) has demonstrated a 56% ORR in patients with ALK^+ lung cancer who have progressed on crizotinib[24]. Yet only a minority of these patients had *ALK* alterations, suggesting the possibility of alternative bypass mechanisms that are sensitive to LDK-378. Notably, LDK-378 and the structurally related ALK inhibitor TAE-684 can inhibit both ALK and

IGF-1R *in vitro*[25]. We hypothesized that the efficacy of LDK-378 may be due to this drug's ability to simultaneously block both ALK and IGF-1R. LDK-378 was more potent than crizotinib in H3122 (**Fig. 6a**), STE-1 (**Supplementary Fig. 7a**) and H3122 XR (**Supplementary Fig. 7b**) cells. LDK-378 was also more potent at inducing apoptosis in H3122 cells (**Supplementary Fig. 7c**). Furthermore, LDK-378 was significantly more effective at delaying the growth of H3122 xenografts compared to the equivalent dose of crizotinib (**Fig. 6b**).

Next we tested LDK-378's ability to inhibit IGF-1R phosphorylation. We treated H3122 (**Fig. 6c**) and H2228 (**Fig. 6d**) cells with LDK-378 alone or in combination with IGF-1. Notably, LDK-378 treatment inhibited ALK phosphorylation and was also able to overcome the IGF-1 ligand–induced increase in IGF-1R phosphorylation in both ALK$^+$ cell lines (**Fig. 6c**,**d**). These data suggest that the potency of LDK-378 *in vivo* may be due to this agent's combined ability to block both ALK and IGF-1R.

DISCUSSION

We report that ALK and IGF-1R inhibitors have cooperative antiproliferative effects. IGF-1R inhibitors sensitized *ALK* fusion–positive lung cancer cells to the effects of ALK inhibition. We observed therapeutic synergism between ALK and IGF-1R inhibitors in both ALK TKI–sensitive and ALK TKI–resistant settings. Chronic ALK inhibition was associated with enhanced IGF-1R signaling. The ALK TKI–resistant cells used numerous mechanisms to activate IGF-1R signaling. Notably, the addition of an IGF-1R inhibitor sensitized the resistant cells to the effects of ALK blockade.

We propose drug combinations co-targeting ALK and IGF-1R as a new therapeutic approach in patients with ALK$^+$ lung cancer. This rationally selected combination of targeted therapies should be effective in both ALK TKI–naive and ALK TKI–resistant settings. Our data may also explain in part the surprising 56% ORR for the second-generation ALK TKI LDK-378 in patients with ALK$^+$ lung cancer who had progressed on crizotinib[24]. As we observed responses to LDK-378 in both patients with and without second-site ALK mutations, the increased on-target potency of LDK-378 toward ALK is by itself not enough to explain all of the responses seen with this agent. We hypothesize that the potency of this agent is due to its ability to simultaneously inhibit both ALK and IGF-1R, and our *in vitro* experiments confirm that LDK-378 does inhibit phosphorylation of both ALK and IGF-1R. Further studies will be necessary to validate this hypothesis in clinical samples.

The mechanisms of acquired resistance to ALK inhibitors are just beginning to be understood. Target alterations in *ALK* have been found in only a minority of resistant tumors examined so far. Bypass signaling has also been reported[3–6]. Notably, target alterations and bypass signaling do not appear to be mutually exclusive. One of the patients in our study had both an ALK G1202R mutation and increased pIGF-1R levels at the time of crizotinib resistance. Previous reports have also documented the co-occurrence of ALK kinase domain mutations with increased EGFR phosphorylation or focal *KIT* amplification in two separate patients with crizotinib resistance[3]. The frequency of the various ALK TKI resistance mechanisms and the degree to which the off-target effects of the ALK TKI may dictate both clinical efficacy and also the mechanism of resistance remain to be more precisely defined.

In conclusion, provoked by observations from an exceptional responder, we have identified the IGF-1R–IRS-1 signaling axis as a potential therapeutic target in ALK$^+$ lung cancer. Because ALK is as an oncogenic driver in a growing number of hematologic and solid organ tumors, an improved understanding of ALK signaling, as well as the mechanisms of escape from ALK inhibition, may have direct therapeutic implications for other ALK-driven malignancies.

METHODS

Methods and any associated references are available in the online version of the paper.

Accession codes. The whole-genome sequencing data from this study can be accessed at the NCBI Sequence Read Archive (SRA; http://www.ncbi.nlm.nih.gov/sra) under accession number SRP044308 (tumor: SRR1514863, and blood: SRR1514948). The microarray data reported in this article have been deposited in NCBI's Gene Expression Omnibus (GEO) database at http://www.ncbi.nlm.nih.gov/geo (accession number GSE49508).

Note: Any Supplementary Information and Source Data files are available in the online version of the paper.

ACKNOWLEDGMENTS

This work was supported by the Vanderbilt-Ingram Cancer Center Core grant (P30-CA68485), a career development award from the Vanderbilt Specialized Program of Research Excellence in Lung Cancer grant (CA90949), US National Cancer Institute grants R01CA121210 and P01CA129243 and the Joyce Family Foundation. C.M.L. was additionally supported by a US National Institutes of Health (NIH) K12 training grant (K12 CA9060625), an American Society of Clinical Oncology Young Investigator Award, a Uniting Against Lung Cancer grant and a Damon Runyon Clinical Investigator Award. C.M.L. was the Carol and Jim O'Hare chief fellow from 7/1/2011 through 6/30/2012. L.C.H. and R.B. were supported by the Deutsche Forschungsgemeinschaft (SFB 832, Tumormicromilieu) and the German Cancer Aid (Center for Integrated Oncology (CIO) Köln-Bonn). M. Bos was supported by the European Regional Development Fund grant number FKZ:005-111-0027. G.M.W. was supported by the Victorian Cancer Agency grant TS10_01. K.-K.W. is supported by the NIH CA122794, CA140594, CA163896, CA166480 and CA154303 grants. P.K.P. was supported by a Uniting Against Lung Cancer grant. R.K.T. is supported by the EU-Framework Programme CURELUNG (HEALTH-F2-2010-258677), the Deutsche Forschungsgemeinschaft through TH1386/3-1 and SFB832 (TP6), the German Ministry of Science and Education (BMBF) as part of the NGFNplus program (grant 01GS08100) and the Deutsche Krebshilfe as part of the Oncology Centers of Excellence funding program. S.P. was supported by a grant from the Rudolph Becker Foundation. J.W. was supported by the German Cancer Aid (CIO Köln-Bonn), the Federal Ministry of Education and Research (NGFNplus) and the Ministry of Economy, Energy, Industry and Craft of North Rhine-Westfalia (NRW) in the PerMed NRW framework program. Z.Z. was supported by NIH R01LM011177. We thank J. Sosman and C. Arteaga for their critical review of this manuscript, C. Liang (Xcovery) for providing X-376 and A. Nashabi for administrative assistance. Australian specimens were processed by the Victorian Cancer Biobank. The human anaplastic lymphoma cell line, SUDHL-1, was a generous gift from S. Morris of St. Jude Children's Research Hospital.

AUTHOR CONTRIBUTIONS

C.M.L. and W.P. conceived the project and wrote the manuscript. C.M.L., N.T.M., Y.Y., H.J. and M.R.-B. performed the molecular biology experiments. H.C., P.L., X.C. and R.S. performed the statistical analyses. S.O.-C., L.C.H., A.F. and R.K.T. performed all the IGF-1R and IRS-1 immunohistochemistry experiments. S.O.-C., L.O., P.K.P., R.B., S.A., S.P., M. Brockmann, M. Bos, J.W., M.G., G.M.W., B.S., P.A.R., T.-M.R. and R.K.T. provided clinical samples. D.H.J. and L.H. provided clinical care for the index patient. Z.C. and K.-K.W. provided the *EML4-ALK* E13;A20 transgenic mice. D.L., L.W., Y.S. and M.L. performed all the FISH and NanoString experiments. R.T. and E.d.S. performed the xenograft studies. Q.W. and Z.Z. analyzed the whole-genome sequencing data.

COMPETING FINANCIAL INTERESTS

The authors declare competing financial interests: details are available in the online version of the paper.

1. Grande, E., Bolos, M.V. & Arriola, E. Targeting oncogenic ALK: a promising strategy for cancer treatment. *Mol. Cancer Ther.* **10**, 569–579 (2011).

2. Camidge, D.R. *et al.* Activity and safety of crizotinib in patients with ALK-positive non-small-cell lung cancer: updated results from a phase 1 study. *Lancet Oncol.* **13**, 1011–1019 (2012).
3. Katayama, R. *et al.* Mechanisms of acquired crizotinib resistance in ALK-rearranged lung cancers. *Sci. Transl. Med.* **4**, 120ra117 (2012).
4. Doebele, R.C. *et al.* Mechanisms of resistance to crizotinib in patients with ALK gene rearranged non-small cell lung cancer. *Clin. Cancer Res.* **18**, 1472–1482 (2012).
5. Lovly, C.M. & Pao, W. Escaping ALK inhibition: mechanisms of and strategies to overcome resistance. *Sci. Transl. Med.* **4**, 120ps122 (2012).
6. Tanizaki, J. *et al.* Activation of HER family signaling as a mechanism of acquired resistance to ALK inhibitors in EML4-ALK–positive non-small cell lung cancer. *Clin. Cancer Res.* **18**, 6219–6226 (2012).
7. Iyer, G. *et al.* Genome sequencing identifies a basis for everolimus sensitivity. *Science* **338**, 221 (2012).
8. Shaw, A.T. *et al.* Clinical features and outcome of patients with non-small-cell lung cancer who harbor EML4-ALK. *J. Clin. Oncol.* **27**, 4247–4253 (2009).
9. Boik, J.C., Newman, R.A. & Boik, R.J. Quantifying synergism/antagonism using nonlinear mixed-effects modeling: a simulation study. *Stat. Med.* **27**, 1040–1061 (2008).
10. Mulvihill, M.J. *et al.* Discovery of OSI-906: a selective and orally efficacious dual inhibitor of the IGF-1 receptor and insulin receptor. *Future Med. Chem.* **1**, 1153–1171 (2009).
11. Metz, H.E. & Houghton, A.M. Insulin receptor substrate regulation of phosphoinositide 3-kinase. *Clin. Cancer Res.* **17**, 206–211 (2011).
12. Yang, X. *et al.* Using tandem mass spectrometry in targeted mode to identify activators of class IA PI3K in cancer. *Cancer Res.* **71**, 5965–5975 (2011).
13. Chen, Z. *et al.* Inhibition of ALK, PI3K/MEK, and HSP90 in murine lung adenocarcinoma induced by EML4-ALK fusion oncogene. *Cancer Res.* **70**, 9827–9836 (2010).
14. Lovly, C.M. *et al.* Insights into ALK-driven cancers revealed through development of novel ALK tyrosine kinase inhibitors. *Cancer Res.* **71**, 4920–4931 (2011).
15. Katayama, R. *et al.* Therapeutic strategies to overcome crizotinib resistance in non-small cell lung cancers harboring the fusion oncogene EML4-ALK. *Proc. Natl. Acad. Sci. USA* **108**, 7535–7540 (2011).
16. Guix, M. *et al.* Acquired resistance to EGFR tyrosine kinase inhibitors in cancer cells is mediated by loss of IGF-binding proteins. *J. Clin. Invest.* **118**, 2609–2619 (2008).
17. Cortot, A.B. *et al.* Resistance to irreversible EGF receptor tyrosine kinase inhibitors through a multistep mechanism involving the IGF1R pathway. *Cancer Res.* **73**, 834–843 (2013).
18. García-Echeverria, C. *et al.* *In vivo* antitumor activity of NVP-AEW541—a novel, potent, and selective inhibitor of the IGF-IR kinase. *Cancer Cell* **5**, 231–239 (2004).
19. Morgillo, F. *et al.* Implication of the insulin-like growth factor-IR pathway in the resistance of non-small cell lung cancer cells to treatment with gefitinib. *Clin. Cancer Res.* **13**, 2795–2803 (2007).
20. Vazquez-Martin, A. *et al.* IGF-1R/epithelial-to-mesenchymal transition (EMT) crosstalk suppresses the erlotinib-sensitizing effect of EGFR exon 19 deletion mutations. *Sci. Rep.* **3**, 2560 (2013).
21. Chmielecki, J. *et al.* Optimization of dosing for EGFR-mutant non-small cell lung cancer with evolutionary cancer modeling. *Sci. Transl. Med.* **3**, 90ra59 (2011).
22. Ohashi, K. *et al.* Lung cancers with acquired resistance to EGFR inhibitors occasionally harbor BRAF gene mutations but lack mutations in KRAS, NRAS, or MEK1. *Proc. Natl. Acad. Sci. USA* **109**, E2127–E2133 (2012).
23. Suehara, Y. *et al.* Identification of KIF5B-RET and GOPC-ROS1 fusions in lung adenocarcinomas through a comprehensive mRNA-based screen for tyrosine kinase fusions. *Clin. Cancer Res.* **18**, 6599–6608 (2012).
24. Shaw, A.T. *et al.* Ceritinib in ALK-rearranged non-small-cell lung cancer. *N. Engl. J. Med.* **370**, 1189–1197 (2014).
25. Galkin, A.V. *et al.* Identification of NVP-TAE684, a potent, selective, and efficacious inhibitor of NPM-ALK. *Proc. Natl. Acad. Sci. USA* **104**, 270–275 (2007).

ONLINE METHODS

Cell culture. All cell lines were maintained in a humidified incubator with 5% CO_2 at 37 °C. The human lung adenocarcinoma cell lines H3122 and H2228 have been described previously and were verified to harbor their reported genetic alterations by direct cDNA sequencing[14]. Derivation of the human lung adenocarcinoma cell line, STE-1, is described below. The human anaplastic lymphoma cell line, SUDHL-1, has been described previously[26]. The isogenic pairs of EGFR TKI–sensitive and EGFR TKI–resistant cell lines used in these studies, including PC-9/PC-9 ERc1, HCC4006/HCC4006 ER, HCC827/HCC827 ER and HCC2279/HCC2279 ER, have been described previously[21,22]. The EGFR TKI–resistant cells (denoted ER for erlotinib resistant) were grown continuously in 1 μM erlotinib. All cell lines were maintained in RPMI 1640 medium (Mediatech, Inc., Manassas, VA, USA) supplemented with 10% heat-inactivated FBS (Atlanta Biologicals, Lawrenceville, GA, USA) and penicillin-streptomycin (Mediatech, Inc., Manassas, VA, USA) to final concentrations of 100 U ml^{-1} and 100 μg ml^{-1}, respectively. All cell lines were routinely evaluated for mycoplasma contamination.

Derivation of the STE-1 cell line. Pleural fluid was obtained with informed consent from a patient with crizotinib-naive ALK^+ metastatic lung adenocarcinoma. After pelleting the cells and washing three times in sterile PBS, red blood cells were lysed in ACK buffer (Lonza INC, Allendale, NJ, USA). After lysis, the remaining cell pellet was washed three times in sterile PBS. The remaining mixture of cells was then distributed into 10-cm dishes. Cells were cultured in RPMI medium supplemented with 10% heat-inactivated FBS and penicillin-streptomycin as described above. The medium was changed every 1–3 d for approximately 3 months. To verify that the established cell line (named STE-1) harbored an *ALK* fusion, *ALK* FISH (**Supplementary Fig. 8a**) and cDNA sequencing (**Supplementary Fig. 8b**) of the *ALK* fusion were performed as described below.

Whole-genome sequencing of the STE-1 cell line. Paired-end sequencing of tumor and matched blood genomic DNA was conducted on an Illumina Genome Analyzer IIx platform. The reads were aligned to the Human Genome (UCSC hg19) using BWA[27]. The default arguments of BWA were applied to the alignment. After the alignment, we ran the software SAMtools[28] to convert the alignment files to a sorted, indexed binary alignment map (BAM) format. Then we used the Picard website (http://picard.sourceforge.net/index.shtml) to mark duplicate reads. To obtain the best call set possible, we also used the software GATK[29] to do realignment and recalibration. The recalibrated alignment files were then used for single-nucleotide variant detection. The sequencing data from this study can be accessed at the NCBI Sequence Read Archive (SRA; http://www.ncbi.nlm.nih.gov/sra) under accession number SRP044308 (tumor: SRR1514863 and blood: SRR1514948 blood).

Generation of TKI-resistant cell lines. To create ALK TKI–resistant lines, parental (TKI-sensitive) cells were cultured with increasing concentrations of TKIs starting with the one-third maximum inhibitory concentration (IC_{30}). Doses were increased in a stepwise pattern when normal cell proliferation patterns resumed. Fresh drug was added every 72–96 h. Resistant cells that grew in 1 μM crizotinib and 4 μM X-376 were derived after approximately 6 months of culturing in the continuous presence of drug. DNA identity testing on both the parental and resistant cells confirmed that the cells were derived from the same origin. Resistant cells were maintained initially as polyclonal populations under constant TKI selection.

Compounds. X-376 was prepared as described previously[14]. Crizotinib (ChemieTek, Indianapolis, IN, USA), OSI-906 (Selleck Chemicals, Houston, TX, USA), AEW-541 (Selleck Chemicals, Houston, TX, USA), LDK-378 (Selleck Chemicals, Houston, TX, USA) and lapatinib (Selleck Chemicals, Houston, TX, USA) were dissolved in DMSO. Erlotinib was synthesized by the Memorial Sloan Kettering Cancer Center (MSKCC) Organic Synthesis Core. mAb391 (R&D Systems, Minneapolis, MN, USA) was dissolved in PBS.

Cell viability, soft agar and apoptosis assays. For viability experiments, cells were seeded in 96-well plates at 25–33% confluency and exposed to drugs alone or in combination the following day. At 72 h after drug addition, Cell Titer Blue reagent (Promega, Madison, WI, USA) was added, and fluorescence was measured on a Spectramax spectrophotometer (Molecular Devices, Sunnyvale, CA, USA) according to the manufacturer's instructions. All experimental points were set up in hextuplicate replicates (except for the data presented in **Fig. 4b**, which was set up in triplicate) and were performed at least three independent times. Data are presented as the percentage of viable cells compared to control (vehicle treatment only) cells. Drug synergism was assessed using the Mix-Low method[9]. For soft agar assays, cells were seeded in 96-well plates and treated with drug according to the manufacturer's instructions (Cell BioLabs, Inc., San Diego, CA, USA). The absorbance at 570 nm was measured 7–9 d after cell seeding and drug treatment on a Synergy MX microplate reader (Biotek, Winooksi, VT, USA). All experimental points were set up in hextuplicate replicates and were performed at least two independent times. Data are presented as the percentage of viable cells compared to control (vehicle treatment only) cells. *P* values were determined with Student's *t* test. For STE-1 apoptosis experiments, cells were seeded in six-well plates at approximately 50% confluency and treated with the indicated inhibitors (one dose of inhibitor only). At 72 h after drug addition, cells were collected, washed in PBS and fixed in 100% ethanol. Fixed cells were stained with PI (working solution: 40 μg ml^{-1} PI plus 3.8 mM sodium citrate in PBS). For H3122 XR apoptosis experiments, cells were seeded in six-well plates at approximately 75% confluency and treated with the indicated inhibitors once every 24 h for a total of three doses. At 72 h after drug addition, cells were collected, washed in PBS and fixed in 100% ethanol. All fixed cells were stained with PI (working solution: 40 μg ml^{-1} PI plus 3.8 mM sodium citrate in PBS). Data were collected on a FACSCantoII (BD Biosciences, San Jose, CA, USA) with FACSDiVa software to collect the data and Winlist software for the analysis (Verity Software House).

Antibodies and immunoblotting. The following antibodies were obtained from Cell Signaling Technology (Danvers, MA, USA): ALK D5F3 (3333, 1:1,000 dilution), ALK 31F12 (3791, 1:1,000 dilution), pALK Y1604 (3341, 1:500–1:750 dilution), ribosomal protein S6 (2317, 1:1,000–1:2,000 dilution), pS6 S240/S244 (5364, 1:5,000–1:6,000 dilution), ERK (9102, 1:2,000–1:3,000 dilution), pERK T202/Y204 (9101, 1:2,000–1:3,000 dilution), AKT (9272, 1:1,000–1:2,000 dilution), pAKT S473 (9271, 1:500 dilution), IGF-1R β (3027, 1:2,000 dilution), pIGF-1R Y1131 (3021, 1:500–1:1,000 dilution), IRS-1 D23G12 (3407, 1:1,000 dilution), horseradish peroxidase (HRP)-conjugated anti-mouse (7076, 1:1,000–1:2,000 dilution) and HRP-conjugated anti-rabbit (7074, 1:1,000–1:2,000 dilution). The actin antibody (A2066, 1:5,000 dilution) was purchased from Sigma-Aldrich (St. Louis, MO, USA).

For immunoblotting and immunoprecipitation, cells were harvested, washed in PBS and lysed in 50 mM Tris-HCl, pH 8.0, 150 mM sodium chloride, 5 mM magnesium chloride, 1% Triton X-100, 0.5% sodium deoxycholate, 0.1% SDS, 40 mM sodium fluoride, 1 mM sodium orthovanadate and cOmplete protease inhibitors (Roche Diagnostics, Indianapolis, IN, USA). Lysates were subjected to SDS-PAGE followed by blotting with the indicated antibodies and detection by Western Lightning ECL reagent (PerkinElmer, Waltham, MA, USA). Select images were quantified using a Bio-Rad Gel Doc XR and Image Lab software (Bio-Rad, Hercules, CA, USA) and normalized to the actin signal. Data are represented as band signal intensity compared to the vehicle-only control. For immunoprecipitation experiments, lysates were incubated with the primary antibody overnight at 4 °C. Protein A Dynabeads (Invitrogen, Carlsbad, CA, USA) were then added and incubated in the lysate for 1 h at 4 °C. Immobilized beads were washed four times with lysis buffer.

cDNA sequencing of ALK. Total RNA was isolated from cell pellets using the RNeasy mini kit (Qiagen, Germantown, MD, USA). The SuperScript III one-step RT-PCR system with platinum Taq DNA polymerase (Invitrogen, Carlsbad, CA, USA) was used to perform both cDNA synthesis and PCR amplification with gene-specific primers: *EML4* E18F (aligned on *EML4* exon 13, 5′-TTAGCATTCTTGGGGAATGG-3′) and *ALK*_kinase domain_R (5′-GCCTGTTGAGAGACCAGGAG-3′). The 1,223-bp PCR product, which includes the *EML4-ALK* fusion point and the entire ALK kinase domain, was sequenced in both directions by Sanger dideoxynucleotide sequencing. Sequencing data confirmed that H3122 parental, H3122 CR, H3122 XR and

STE-1 cells all harbored the *EML4-ALK* E13;A20 (variant 1) fusion and that H2228 harbored the *EML4-ALK* E6a/b;A20 (variant 3) fusion. No kinase domain mutations were found in any of these cell lines compared with *Homo sapiens* mRNA for *EML4-ALK* E13;A20 variant 1 (GeneBank: AB274722.1).

RTK proteome array and IGF-1 ELISAs. Proteome Profiler Human Phospho-RTK Array Kits (R&D Systems, ARY001B) and human IGF-1 Quantikine ELISA kits (R&D Systems, DG100) were processed according to manufacturer protocols.

siRNA experiments. Cells were reverse transfected with siRNAs using the Lipofectamine RNAimax reagent (Life Technologies, Grand Island, NY, USA). Nontargeting and IRS-1 siRNAs pools were purchased from Dharmacon (Lafayette, CO, USA) and Santa-Cruz (Dallas, TX, USA).

NanoString nCounter analysis. NanoString nCounter analysis of RNA isolated from formalin-fixed and paraffin-embedded (FFPE) samples was performed as described previously[23]. The raw data were normalized to the nCounter system spike-in positive and negative controls in each sample. The normalized results are expressed as the relative mRNA level. The comparison between groups before and after treatment was performed by modified paired *t* test using the limma package.

FISH. Samples were tested for *ALK* rearrangements by FISH (Vysis ALK Break Apart FISH Probe Kit) as described previously[30].

Gene expression analysis. RNA from cell lines and controls was prepared, labeled and hybridized to the Illumina HT-12 array. For analysis, the sample probe profile data in the GeneSpring export format was transformed to the $\log_2$ scale and normalized using the quantile method by applying the beadarray package[31] in BioConductor 2.11. Four duplicated samples were averaged to reduce the total sample size to nine across three groups. The comparison between drug-sensitive and drug-resistant groups was performed using the limma package. The significantly changed probes were identified by moderated *t* statistics. The *P* values from moderated *t* tests were adjusted by Benjamini and Hochberg's method to control the false discovery rate. The microarray data reported in this article have been deposited in NCBI's Gene Expression Omnibus (GEO) database at http://www.ncbi.nlm.nih.gov/geo (accession number GSE49508).

Xenograft studies. Nude mice (*nu/nu*; Harlan Laboratories) were used for *in vivo* studies and were cared for in accordance with guidelines approved by the Memorial Sloan Kettering Cancer Center Institutional Animal Care and Use Committee (IACUC) and Research Animal Resource Center. 8-week-old female mice were injected subcutaneously with 5 million H3122 cells together with Matrigel. Once tumors reached an average volume of 100 mm^3, mice were randomized to the different treatment cohorts. For the experiment presented in **Supplementary Figure 1f**, mice were randomized to receive either crizotinib alone, mAb391 alone, crizotinib plus mAb391 or vehicle control ($n = 6$ for vehicle alone, crizotinib and crizotinib plus mAb391; $n = 5$ for mAb391 only). Crizotinib was administered at 50 mg per kg body weight p.o. daily for 5 d. mAb391 was administered at 1 mg intraperitoneally (i.p.) every 3 d. For the experiment presented in **Figure 6b**, mice were randomized to receive crizotinib alone (50 mg per kg body weight p.o. daily for 5 d), LDK-378 alone (50 mg per kg body weight p.o. daily for 5 d) or vehicle control ($n = 5$ for crizotinib and LDK-378, $n = 4$ for vehicle control). Mice were observed daily throughout the treatment period for signs of morbidity and/or mortality. Tumors were measured twice weekly using calipers, and tumor volume was calculated using the formula length × width^2 × 0.52. Body weight was also assessed twice weekly. *P* values were determined with the Wilcoxon rank-sum test.

***EML4-ALK* E13;A20 transgenic mice.** Genetically engineered mice harboring the *EML4-ALK* E13;A20 fusion variant have been reported previously[13]. Three-month-old mice of both genders were used in the studies described. All animal treatment studies were reviewed and approved by the IACUC at the Dana-Farber Cancer Institute.

Tumor biopsy samples. All patient tumor biopsy samples were obtained under Institutional Review Board (IRB)-approved protocols (Vanderbilt University IRB# 050644, Memorial Sloan Kettering Cancer Center IRB #10-136, University Hospital of Cologne IRB #06037 and Peter MacCallum Cancer Center IRB#08/71). Written informed consent was obtained from all patients. All samples were deidentified, and protected health information was reviewed according to Health Insurance Portability and Accountability Act (HIPAA) guidelines. For the index patient's tumor, clinical genotyping was performed using the SNaPshot platform as described previously[32].

Clinical trial information. The index patient was enrolled in a phase 1/2a clinical trial of erlotinib followed at progression by erlotinib plus the IGF-1R monoclonal antibody, MK-0646, in patients with recurrent non–small cell lung cancer (NCT00654420).

IHC. Tumors were pathologically identified and classified according to World Health Organization guidelines. Briefly, 3-µm-thick sections of FFPE tumors were deparaffinized. For pIGF-1R staining, antigen retrieval was performed by boiling the section in citrate buffer at pH 6 for 25 min. For IRS-1 staining, no pretreatment was necessary. The primary antibodies used were as follows: pIGF-1R (Y1161) (Ab39398, 1:100, pH 6, Abcam Inc.) and IRS-1 (Ab40777, 1:100, Abcam Inc.). Corresponding secondary antibodies and detection kits were used (Enhancer: post antibody blocking for Bright Vision plus; Immuno Logic c-DPVB blocking and Polymer: Poly-HRP-GAM/R/R IgG; Immuno Logic c-DPVB999HRP, BrightVision+ cat #DPVB999HRP, ImmunoLogic, Duiven, the Netherlands, http://www.immunologic.nl) and stained on an automated stainer (LabVision Autostainer 480S, Thermo Scientific). Staining intensities were individually evaluated by three independent observers.

26. Morris, S.W. *et al.* Fusion of a kinase gene, ALK, to a nucleolar protein gene, NPM, in non-Hodgkin's lymphoma. *Science* **263**, 1281–1284 (1994).
27. Li, H. & Durbin, R. Fast and accurate short read alignment with Burrows-Wheeler transform. *Bioinformatics* **25**, 1754–1760 (2009).
28. Li, H. *et al.* The Sequence Alignment/Map format and SAMtools. *Bioinformatics* **25**, 2078–2079 (2009).
29. McKenna, A. *et al.* The Genome Analysis Toolkit: a MapReduce framework for analyzing next-generation DNA sequencing data. *Genome Res.* **20**, 1297–1303 (2010).
30. Gainor, J.F. *et al.* ALK rearrangements are mutually exclusive with mutations in EGFR or KRAS: an analysis of 1,683 patients with non-small cell lung cancer. *Clin. Cancer Res.* **19**, 4273–4281 (2013).
31. Dunning, M.J., Smith, M.L., Ritchie, M.E. & Tavare, S. Beadarray: R classes and methods for Illumina bead-based data. *Bioinformatics* **23**, 2183–2184 (2007).
32. Su, Z. *et al.* A platform for rapid detection of multiple oncogenic mutations with relevance to targeted therapy in non-small-cell lung cancer. *J. Mol. Diagn.* **13**, 74–84 (2011).

doi:10.1038/nm.3667